Characterization of K-mixed V_2O_5 catalyst and oxidative dehydrogenation of propane on it

Takehiko Ono [a,*], Yuhmo Tanaka [a], Takayoshi Takeuchi [b], Kouji Yamamoto [b]

[a] *Department of Environmental Science and Technology, Sinshu University, 4-17-1 Wakasato, Nagano 380-8553, Japan*
[b] *Department of Applied Chemistry, Osaka Prefecture University, 1-1 Gakuen-cho, Sakai, Osaka 599-8531, Japan*

Abstract

The structure of K containing V_2O_5 catalysts has been studied by XRD and spectroscopic methods. The particles of V_2O_5 were oriented sharply to the direction perpendicular to b axis. The spacings of (010) and (200) planes were slightly contracted by the presence of K ions. V_2O_5 bronze seemed to be less Raman-active. IR spectra gave the structural information of K-V_2O_5 at low content of K. The IR bands at 1023 and 830 cm^{-1} of V_2O_5 shifted to 1000 and 785 cm^{-1}, respectively. This suggests that K ions are present at some micro space of V_2O_5 crystal. The K-V_2O_5 catalyst oriented to (010) plane exhibited high selectivity (ca. 80%) to C_3H_6 in the oxidation of C_3H_8 while the activity decreased with the increase in K content. Oxygen ions of oriented V_2O_5 were exchanged with ^{18}O by the reduction with C_3H_8 and reoxidation with $^{18}O_2$. Raman spectra's analysis of the catalysts exchanged with ^{18}O suggests that V=O species are responsible for oxidative dehydrogenation of C_3H_8 to C_3H_6. © 2000 Elsevier Science B.V. All rights reserved.

Keywords: V_2O_5 catalyst; Propane; IR spectra

1. Introduction

The oxidative dehydrogenation of alkane has been studied since it is a potential process for alkenes production. Supported vanadia catalysts have been often used for the oxidative dehydrogenation and these have been prepared with alkali or alkali earth metal oxides [1–5]. The K containing V_2O_5 catalysts had been used for oxidation of SO_2 and studied by many workers in the past [6–10]. The vanadium pentoxide gives bronzes with Li and Na cations. However, only some small amounts of K ions have been introduced to V_2O_5 [11,12]. There have been some IR and Raman spectroscopic studies with K-V_2O_5 catalysts [8,13–15]. In this work, the role of K addition on V_2O_5 structure has been studied using IR and Raman spectroscopies. The oxidative dehydrogenation of propane over V_2O_5 catalysts doped with K ions has been also studied. The oxygen species responsible for oxidation on V_2O_5 catalyst have been studied previously by one of the authors using ^{18}O tracer

* Corresponding author. Tel.: +81-26-269-5532; fax: +81-26-269-5550.
E-mail address: takeono@gipwc.shinshu-u.ac.jp (T. Ono).

and Raman spectroscopy [16–18]. Those responsible for oxidative dehydrogenation on K-V_2O_5 have been studied using ^{18}O tracer in this work.

2. Experimental

2.1. Materials

The K containing V_2O_5 catalysts were prepared by two methods. The A series is as follows: the desired amount of KOH solution (K 0.01–2 at.%:100 K/(K + V)) was impregnated on V_2O_5 (Kishida in Japan, 2 m^2/g) and they were heated at 873 K. The B series is as follows: the desired amounts of NH_4VO_3 (Kishida) and KNO_3 (K 5–20 at.%:100 K/(K + V)) were mixed and heated at 873 K for 5 h. The resulting catalyst mass was crashed and powdered. The oriented V_2O_5 catalyst without K ions was prepared by heating V_2O_5 at 973 K above its melting point. The reactant gas C_3H_8 (99.9%) was obtained from Takachiho. The O_2 (99%) gas was obtained from cylinder. The $^{18}O_2$ (98 at.%) was obtained from Isotec (USA)

2.2. Procedures

The structure of catalysts was studied by using XRD (Rigaku-denki), IR (Perkin Elmer 1600) and laser Raman (Jasco NR-1000) spectroscopies. The IR spectra were measured by usual KBr method. The peak-shape analysis of IR bands was provided at Perkin Elmer Japan in Osaka. The oxidative dehydrogenation of propane was carried out using a closed circulation system(ca. 380 cm^3). The products were analyzed by gas chromatography. The Raman spectra of V_2O_5 exchanged with ^{18}O tracer via redox reaction were measured. An Ar-ion laser was tuned to the 514.5 nm line for excitation and its power was set at 200–250 mW. The technique in the peak-shape analysis of Raman

spectra reported by Miyata et al. [19,20] was used.

3. Results and discussion

3.1. Characterization of K-V_2O_5 catalysts

The surface areas were decided by N_2 adsorption as 2, 1.35, 0.58, 0.55, and 0.4 m^2/g for the A catalysts that contain 0, 0.01, 0.1, 0.25, and 0.5 at.% of K ions, respectively. The results of X-ray diffraction for the A catalysts are shown in Fig.1. Fig. 1a shows the diffraction lines of V_2O_5 itself and of K-V_2O_5 containing 0.5 at.% of K. The remarkable increase took place in the intensities of (010) and (020) diffraction lines for the K containing catalyst. The Miller indices reported by Bystrom et al. [21] are used here, whose lattice constants for *b* and *c* axis are reversed from those of JCPDS 9-387. Fig. 1b shows the intensity ratio of (010) and (400) diffraction lines as a function of K content. The results shows remarkable decrease in its ratio by one order. This suggests that the addition of a small amount of K ions from 0.1 to 2 at.% causes to melt V_2O_5 at around 873 K
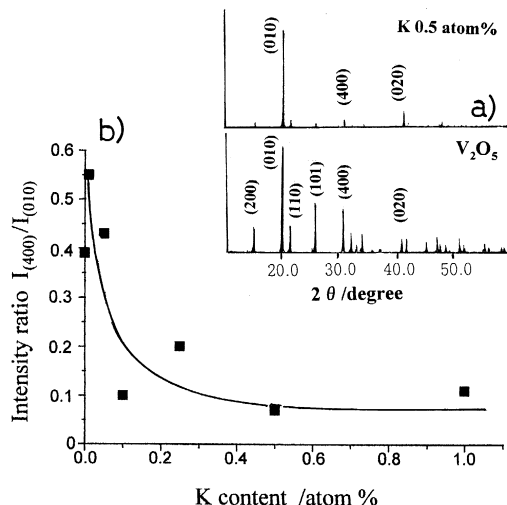

Fig. 1. X-ray diffraction results of the A catalysts. (a) V_2O_5 and K-V_2O_5; (b) The intensity ratio of (400) vs (010). The Miller indices by Bystrom et al. [21] are used.

and that V_2O_5 crystal particles oriented sharply to the direction perpendicular to *b* axis, i.e., the selective exposure of (010) plane. Furthermore, some diffraction angles increased slightly. For example, the spacing of (010) planes was contracted slightly from 0.4380 to 0.4360 nm by the presence of 0.25–1 at.% of K ions. That of (200) planes was also contracted slightly in a similar manner. But those of (002) and other planes were less changed. The addition of more amounts (5–10%) of K ions in the B catalysts showed only V_2O_5 diffraction lines. As shown in Fig. 2, the catalyst of 20 at.% brings about the disappearance of V_2O_5 lines while some small lines appeared. New lines have been assigned to $K_2V_8O_{21}$ [22]. With K5 and K10, the slight contraction such as for (010) spacing of V_2O_5 was observed as the same as in the A catalysts. The K-V_2O_5 in the K20 seems to be X-ray amorphous since the diffraction lines of V_2O_5 disappeared.

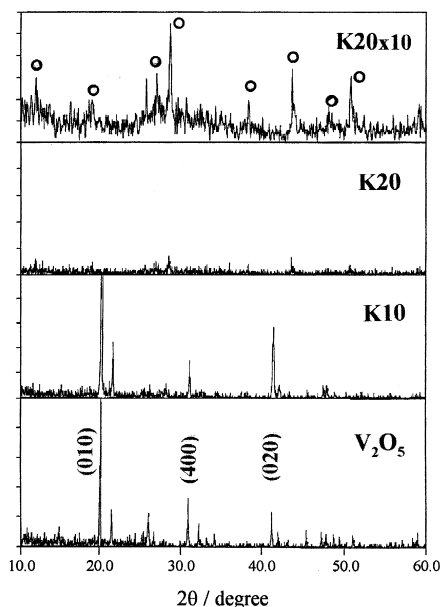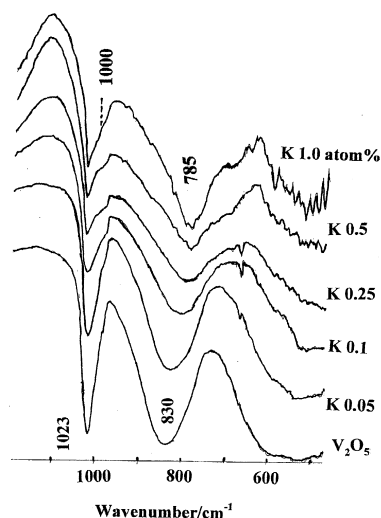The results of IR spectra for the A catalysts are shown in Fig. 3. The bands at 1023 and

Fig. 3. IR spectra of the A catalysts at low K content from 0 to 1.0 at.%.

830 cm^{-1} are assigned to those of V_2O_5 [8, 16]. Their positions change with the addition of 0.05–1 at.% of K ions, i.e., the band at 830 cm^{-1} shifts to 785 cm^{-1} and some shoulder at 1000 cm^{-1} appears. With the B catalysts in Fig. 4, the bands at 1023 and 830 cm^{-1} shift to 1000 and 785 cm^{-1}, respectively, as observed for A catalysts. These shifted bands seem to be attributed to K-mixed compounds such as $K_xV_2O_5$ α bronze ($x < 0.01$) (11). Very small bands appear newly at around 960 cm^{-1} for the 20% catalyst in the B series as shown in Fig.4, which may be those of $K_2V_8O_{21}$ or $K_xV_2O_5$ β such as $K_{0.33-0.25}V_2O_5$ [11].

Fig. 2. X-ray diffraction results of the B catalysts; V_2O_5, K10 (10 at.% of K), K20 (20 at.% of K), and magnified K20 (○: lines of $K_2V_8O_{21}$).
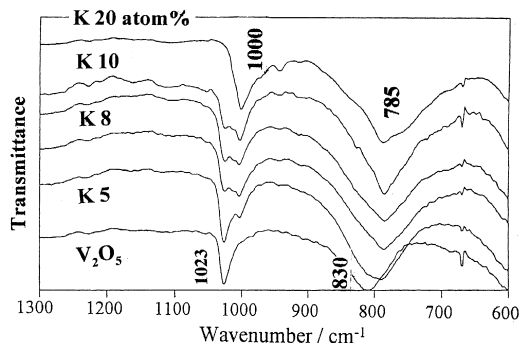

Fig. 4. IR spectra of the B catalysts at high K content from 5 to 20 at.%.

Raman spectra of the A catalysts are shown in Fig. 5. The bands at 1000, 705, and 530 cm^{-1} are those of V_2O_5 [16] The addition of K ions, however, brings about no shift for the spectra of V_2O_5 in the range from 0.01 to 1 at.% of K. The B catalysts, which contain 5–20% of K also showed the bands of V_2O_5 and new bands at 890, 790, and 310 cm^{-1}. New bands seemed to be originated from $K_2V_8O_{21}$, which was assigned by X-ray diffraction. No shift to lower frequencies of V_2O_5 in Raman spectra for both A and B catalysts indicates that the K-mixed phase such as $K_xV_2O_5$ α [11] at low content of K is less Raman-active and seems to be less crystalline.

A peak-shape analysis was attempted with these IR spectra and the shifted fractions were obtained for the catalysts at low contents of K ions. Fig. 6 shows the example of peak-shape analysis of absorbance spectra for the catalyst of 5 at.% of K ions shown in Fig. 4. With the results in Fig. 6, it was assumed that 1023 cm^{-1} shifts to 1000 cm^{-1} and 830 cm^{-1} to 785 cm^{-1} and that the half widths were nearly the same for the two bands separated. Then curve fitting was done between the summed spectra and original spectra. The shifted fractions were calculated from peak area. As shown in Fig. 7, the
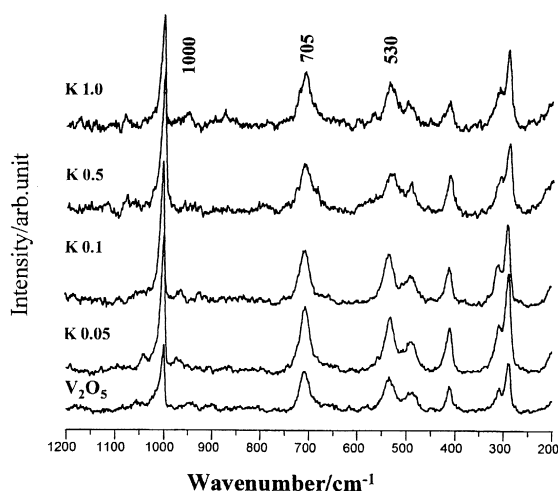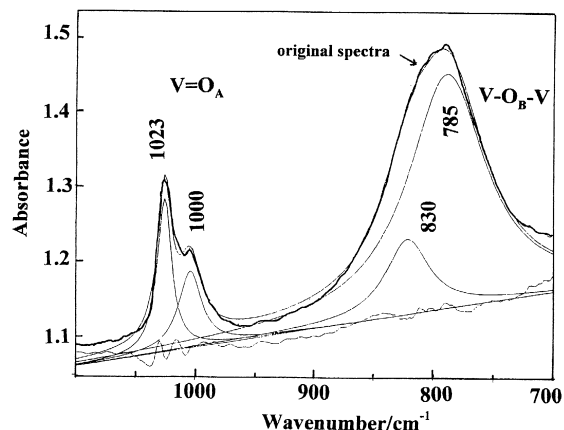

Fig. 6. The peak shape analysis of the B catalyst containing 5 at.% of K after changing to absorbance spectra of K5 in Fig. 4.

tendency of 1023 cm^{-1} band reach to ca. 0.5 in the range from 0.1 to 5 at.% of K ions while that of 830 cm^{-1} band reach to ca.1 at lower content. It is interesting that some difference were found between them. According to previous reports [11,12], the formation of $K_xV_2O_5$ α bronze is limited below 1% of K ions. This seems to arise from similar sizes of K and O ions. Fig. 8 shows the peak area of absorbance for each band as a function of K content for A catalysts. It decreases sharply with the increase of K content, indicating that IR transmission decreases remarkably due to the free electrons at the conduction band such as of n-type semi-
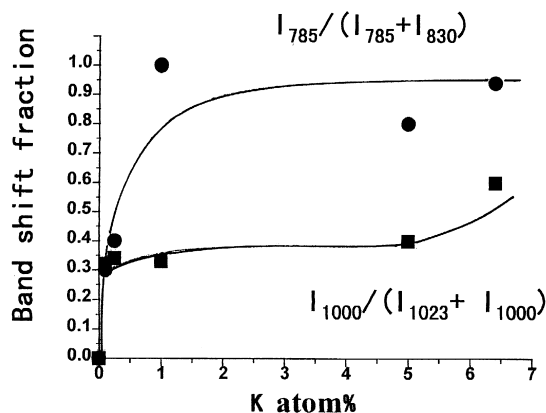

Fig. 5. Raman spectra of the A catalysts at low K contents from 0 to 1.0 at.%.

Fig. 7. Shift fractions of IR bands at 1023 cm^{-1} ($V = O_A$) and 830 cm^{-1} ($V–O_B–V$) as a function of K content for some A and B catalysts.
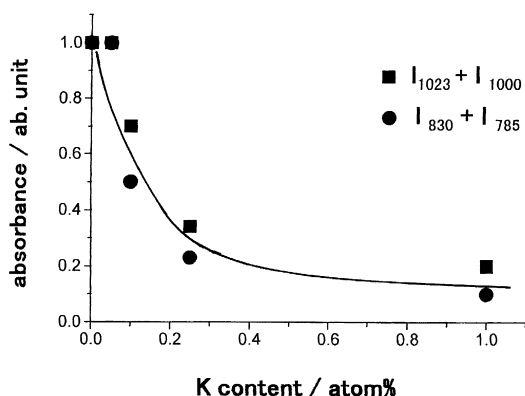
Fig. 8. Absorbance (peak area of Fig. 7) of the IR bands at 1023 and 830 cm^{-1} as a function of K contents for the A catalysts. A comparison can be allowed since the concentrations of V_2O_5 and K containing catalysts in KBr pellet were nearly the same.

conductor. The introduction of K^+ ions to V_2O_5 seem to produce V^{4+} ions and electrons in the conduction band. A remarkable decrease in IR transmission for a n-type semiconductor such as Sn–Sb oxide system was also found [23].

3.2. Structure of K-V_2O_5 catalysts

With the A catalysts, it is demonstrated that the addition of very small amount of KOH cause to melt V_2O_5 catalyst and to form partly K-V_2O_5 bronze such as $K_xV_2O_5$ α [11]. A model of V_2O_5 structure are shown in Fig. 9. Abello et al. [24] have assigned to normal stretching modes for IR bands at 1023 cm^{-1} (double bond, V=O_A) and 830 cm^{-1}(bridge, V–O_B–V) and for Raman bands at 999 cm^{-1}(V=O_A), 700 cm^{-1}(V–O_C–V in V square), and 532 cm^{-1}(bridge, V–O_B). Similar assignments have been reported by Beattie and Gilson [25] as discussed previously [16]. The presence of K ions seems to affect to the V–O vibrations via dipole interactions since the bands at 1025 and 830 cm^{-1} shifted to lower frequencies without remarkable change of spectrum patterns. K ions seem to be inserted in the micro space near O_A along c axis (top of Fig. 9) and near O_B along b axis (bottom of Fig. 9). It seems that K ions are present ca.2 times more

near O_B sites than near O_A sites according to the results in Fig. 7. IR spectrum by KBr method gives generally a bulk information like X-ray diffraction. It is unreasonable that only 0.1–1 at.% of K ions cause to shift the bands of bulk V_2O_5. As far as the A catalysts are concerned, IR information seems to come from several layers of K-V_2O_5 particles since K ions are difficult to enter into bulk due to its size.

With the B catalysts, the structure below 5 at.% of K should be the same as that of the A catalysts described above. The catalysts above 10 at.% of K seem to consist of oriented V_2O_5, K-V_2O_5 bronze such as $K_xV_2O_5$ α, and $K_2V_8O_{21}$. These were characterized by XRD, IR and Raman spectra.

3.3. Catalytic activity and selectivity in propane oxidation over K containing V_2O_5 catalysts

The activity and selectivity in the oxidative dehydrogenation of propane on V_2O_5 and K-V_2O_5 as a function of K content are shown in Fig. 10 for the A catalysts. The selectivity to propene increases to ca. 80% in the range of K content from 0.05 to 1 at.% while the activity
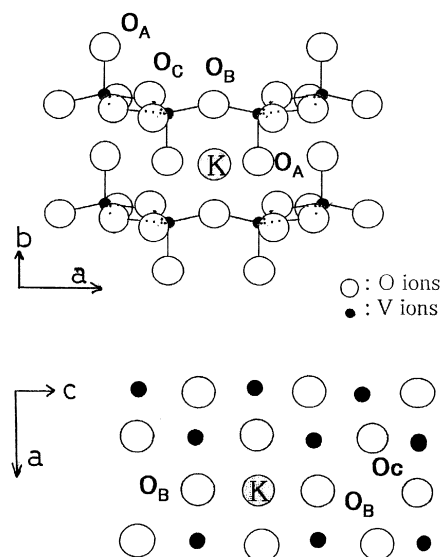

Fig. 9. Structure models of V_2O_5 crystals. O_A, O_B, and O_C denote the oxygen ions of double (terminal) bond, bridged one, and V square one , respectively. K denotes potassium cations.
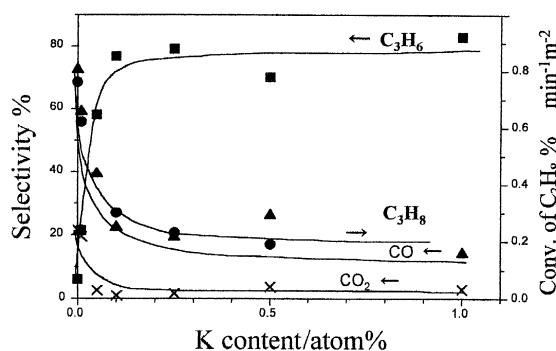
Fig. 10. Rate of conversion in the oxidative dehydrogenation of C_3H_8 and product selectivity over $K-V_2O_5$ catalysts (A catalysts) as a function of K contents. Reaction temp.: 773 K, $p(C_3H_8) = p(O_2) = 15$ Torr (1 Torr = 133.3 Pa), and catalyst: 0.5 g.

Fig. 12. Pressure dependence for oxidative dehydrogenation of C_3H_8 over $K-V_2O_5$ catalyst containing 0.1 at.% of K ions. Reaction temperature 773 K, (●) at 15 Torr of O_2, (X) at 15 Torr of C_3H_8, catalyst: 0.5 g, and the selectivities to C_3H_6 are ca. 80%.

decreases with the K content by one order. Over the B catalysts, similar results were obtained in the range of K content from 5 and 20 at.%. Fig. 11 shows the selectivity to propene as a function of conversion of propane over the A, B, and non-oriented V_2O_5 catalysts. The selectivity over non-oriented V_2O_5 catalyst exhibits only several percent at 20% of conversion. It increases to high value at low conversions. Its selectivity seems to reach above 50–60% at 2–3% of conversion by the extrapolation. The B catalysts exhibit 30–50% of selectivity at 3–9% of conversion. It is concluded that the high selectivity over the $K-V_2O_5$ (A) catalysts comes
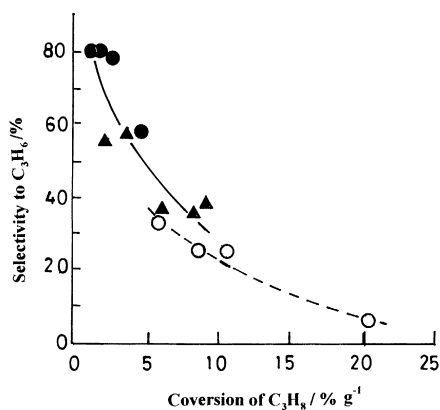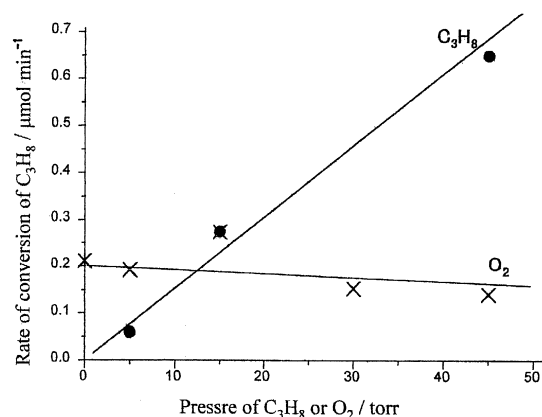

Fig. 11. Selectivity to C_3H_6 over non-oriented V_2O_5 (○), oriented A catalysts (●), and oriented B ones (▲) as a function of conversion of C_3H_8 at 773 K. Reaction times: 10–30 min. Catalyst: 0.5–1 g. Other conditions are the same as in Fig. 10.

mainly from low conversion and from its low activity in consecutive oxidation of propene to CO and CO_2.

According to the characterization of structure for the A catalysts, the catalyst without K ions consisted of non-oriented V_2O_5 particles while the K containing catalysts consisted of V_2O_5 particles oriented to (010) plane and $K-V_2O_5$ bronze. The high selectivity of 80% to propene comes from oriented V_2O_5 and $K-V_2O_5$ bronze species though its activity becomes lower. Fig. 12 shows the pressure dependence over the catalyst with 0.1 at.% of K for the oxidative dehydrogenation of propane. The reaction is first order in C_3H_8 at constant O_2 pressure and zero order in O_2 at constant C_3H_8 pressure. According to a simple redox mechanism [26], the reaction of propane with lattice oxygen is slow while the oxygen insertion to anion vacancies from gaseous oxygen is rapid. In this case, it seems that the first hydrogen abstraction from propane is rate determining as in the case of the oxidation of olefin over oxide catalysts [27].

3.4. Oxygen species responsible for the dehydrogenation of propane using ^{18}O tracer

The catalyst oxygen of oriented V_2O_5 was exchanged with ^{18}O via reduction with C_3H_8

and reoxidation with $^{18}O_2$ by repeating many times. Fig. 13 shows Raman spectra of oriented V_2O_5 and K-V_2O_5 exchanged with ^{18}O. The bands at 999 cm^{-1} and 700 cm^{-1} correspond to V=O$_A$, and V–O$_C$–V stretching vibrations, respectively. The shifted band at 965 cm^{-1} from 999 cm^{-1} appears. The shifted band at 685 from 700 cm^{-1} is difficult to find. Previously [16,18], we reported that the Raman band of V_2O_5 at 999 cm^{-1} shifted to 965 cm^{-1} and that at 702 cm^{-1} to 685 cm^{-1} after the sufficient exchange with ^{18}O. The separated bands by the peak-shape analysis are also shown in Fig. 13. The shift fractions in Table 1 are two to three times larger for V=O$_A$ species than that for V–O$_C$. The results indicate that the oxidative dehydrogenation takes place at V=O$_A$ rather than at V–O$_C$. The high selectivity to propene

Table 1
Shift fractions of Raman spectra over oriented V_2O_5 and non-oriented V_2O_5

	Shift fractions (%)	
	V=O$_A$ (999 cm^{-1})	V–O$_C$ (703 cm^{-1})
This work[a]		
V_2O_5 oriented	18	9
V_2O_5 oriented K 0.1 at.%	6	3
Previous work[b]		
V_2O_5/SiO$_2$ non-oriented	9–16	27

[a] From Fig. 13.
[b] From Ref. [16]. Reduction by *n*-butane and reoxidation by $^{18}O_2$. Average ^{18}O exchange % were 4–6% of V_2O_5 at 710–731 K and the selectivities to $C_4H_6 + C_4H_8$ were 65–70%.

should originate from V=O$_A$, i.e., the selective exposure of the (010) plane. The information of V=O of K$_x$V$_2$O$_5$ bronze itself could not be obtained separately in this work. Its activity for the oxidation may be similar to or below that of V=O$_A$ since both oriented V_2O_5 and its bronze are present in the particles.

As shown in the Table 1, the results in this work are compared with the results over non-oriented V_2O_5 in previous work [16]. In the case of non-oriented V_2O_5 supported on silica , the vacancies of V–O$_C$ species seem to be responsible for reoxidation and the species seem to be responsible for the oxidation of *n*-butane preferentially. In other words, the V=O$_A$ species are less active for the oxidation of *n*-butane. The differences in this work may originate from an activity difference of oxygen species such as O$_A$, O$_C$, and O$_B$ and from how many these species exposes at the catalyst surface. Their nature for oxidative dehydrogenation to propene, however, seem to be less different from each other at low conversion. The high selectivity to propene on K-V_2O_5 catalysts in this work comes from V=O isolation and its low activity.

Some workers reported that V=O oxygen is responsible for oxidation reaction over V_2O_5 catalysts in the past [8,29] while that V–O–V oxygen is responsible for it over V_2O_5/Al$_2$O$_3$ catalyst recently [3]. We previously studied over
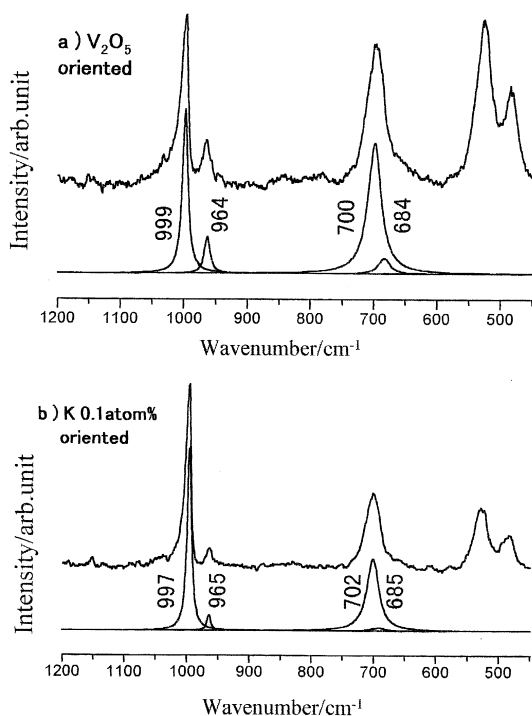

Fig. 13. Peak shape analysis of Raman bands of oriented V_2O_5; (a) and oriented K-V_2O_5 (b), which were exchanged with ^{18}O. 0.1–0.05 g of catalysts were reduced with C_3H_8 (15 Torr) and reoxidized with $^{18}O_2$ (22–30 Torr) at 773–803 K repeatedly for 8–15 times. The selectivity to C_3H_6 in the reduction was ca. 85% in both (a) and (b). The oriented V_2O_5 (a) without K ions was obtained separately by heating at 973 K (see text).

non-oriented MoO_3 catalyst [28] that the vacancies of Mo–O species, which have middle distances were active sites for oxygen insertion while the vacancies for the shortest Mo=O were less active for oxygen insertion. We suggested that Mo=O species were not more active for the oxidation of but-1-ene. The features concerning such oxygen species responsible for oxidation reaction seem to change according to reactants and catalyst conditions.

4. Conclusions

K-V_2O_5 catalysts in the presence of 0.1–2 at.% of K ions were melted even at 873 K. After recrystallization, V_2O_5 particles sharply oriented to the direction perpendicular to *b* axis, i.e., the selective exposure of (010) plane. The spacings of (010) and (200) planes were slightly contracted by the presence of K ions.

According to peak shape analysis of IR spectra, K ions seems to be present at two kinds of micro space of V_2O_5 crystal. The one is near O_A along *c* axis (top of Fig. 9) and the other one is near O_B along *b* axis (bottom of Fig. 9). K ions seem to be present at these sites of the surface of V_2O_5, i.e., K-V_2O_5 bronze particles.

According to peak shape analysis of Raman spectra of the catalysts exchanged with ^{18}O, the oxidative dehydrogenation from C_3H_8 to C_3H_6 seems to take place on V=O_A on oriented K-V_2O_5 catalysts. A comparison of this work and previous work suggests that the activity over (010) plane or by O_A species is lower than other planes such as O_C species while the selectivity to C_3H_6 over (010) or by O_A species becomes higher due to its low activity to consecutive reaction.

References

[1] E.A. Mamedov, V.C. Corberan, Appl. Catal., A 127 (1995) 1.
[2] H.H. Kung, Adv. Catal. 40 (1994) 1.
[3] J.G. Eon, R. Olier, J.C. Volta, J. Catal. 145 (1995) 318.
[4] A. Burrows, C.J. Kiely, J. Perregaard, P.E. Hϕjlund-Nielsen, G. Vorbeck, J.J. Calvino, C. Lopez-Cartes, Catal. Lett. 57 (1999) 121.
[5] A. Kohodakov, B. Olthof, A.T. Bell, E. Iglesia, J. Catal. 181 (1999) 205.
[6] R. Kiyoura, Ryusan 2 (1949) 223, (Japanese).
[7] G.H. Tandy, J. Appl. Chem. 6 (1956) 68.
[8] K. Tarama, S. Teranishi, S. Yoshida, N. Tamura, Proc. 3rd Intern. Congr. Catal., I-8, Amsterdam (1964) 287.
[9] A. Kato, Y. Goto, S. Kawazoe, S. Wada, T. Seiyama, Nippon Kagaku Kaishi 90 (1969) 1212.
[10] G.K. Boreskov, L.P. Daydova, V.M. Mastikhin, G.M. Polykova, Dokl. Phys. Chem. Eng. Ed. 171 (1966) 760.
[11] M. Pouchard, P. Hagenmuller, Mater. Res. Bull. 2 (1967) 799.
[12] P. Hagenmuller, Prog. Solid State Chem. 5 (1971) 71.
[13] A. Tawfik, J. Mater. Sci. Lett. 7 (1988) 1101.
[14] C. Julien, I. Ivanov, A. Gorenstein, Mater. Sci. Eng., B 33 (1995) 168.
[15] S. Takenaka, T. Tanaka, T. Yamazaki, T. Funabiki, S. Yoshida, J. Phys. Chem. B 101 (1997) 9035.
[16] T. Ono, H. Numata, J. Mol. Catal. A: Chem. 116 (1997) 421.
[17] H. Numata, T. Ono, J. Mol. Catal. A: Chem. 130 (1998) 261.
[18] T. Ono, Current Topics in Catalysis 1 (1997) 107, (India).
[19] H. Miyata, K. Fujii, S. Inui, Y. Kubokawa, Appl. Spectrosc. 41 (1986) 1177.
[20] H. Miyata, S. Tokuda, T. Yoshida, Appl. Spectrosc. 43 (1989) 522.
[21] A. Bystrom, K.A. Wilhelmi, O. Brozen, Acta Chem. Scand. 4 (1950) 1119.
[22] JCPDS 21-0711, 39-0889, and 12-0678.
[23] T. Ono, T. Yamanaka, Y. Kubokawa, M. Komiyama, J. Catal. 109 (1988) 423.
[24] L. Abello, E. Husson, Y. Repelin, G. Lucazeau, Spectrochim. Acta., Part A 39 (1983) 64.
[25] L.R. Beattie, T.R. Gilson, J. Chem. Soc. A (1969) 2322.
[26] P. Mars, D.W. VanKrevelen, Chem. Eng. Sci. Suppl. 3 (1955) 41.
[27] T.P. Snyder, C.G. Hill Jr., Catal. Rev.-Sci. Eng. 31 (1989) 43.
[28] T. Ono, H. Numata, N. Ogata, J. Mol. Catal. A: Chem. 105 (1996) 31.
[29] M. Inomata, A. Miyamoto, Y. Murakami, J. Catal. 62 (1980) 140.